Epidural needle with embedded optical fibers for spectroscopic differentiation of tissue: *ex vivo* feasibility study

Adrien E. Desjardins,[1] Benno H.W. Hendriks,[1] Marjolein van der Voort,[1] Rami Nachabé,[1] Walter Bierhoff,[1] Guus Braun,[1] Drazenko Babic,[2] James P. Rathmell,[3] Staffan Holmin,[4] Michael Söderman,[4] and Björn Holmström[5,*]

[1]*Philips Research, Minimally Invasive Healthcare Department, The Netherlands*
[2]*Philips Healthcare, Best, The Netherlands*
[3]*Department of Anesthesia, Critical Care and Pain Medicine, Massachusetts General Hospital/Harvard Medical School, Boston, USA*
[4]*Department of Clinical Neuroscience, Karolinska Institutet and Department of Neuroradiology, Karolinska University Hospital, Solna, Stockholm, Sweden*
[5]*Department of Anesthesiology and Intensive Care, Karolinska University Hospital, Huddinge and Department of Clinical Science, Intervention and Technology, Karolinska Institutet, Stockholm, Sweden*
**bjorn.holmstrom@karolinska.se*

Abstract: Epidural injection is commonly used to provide intraoperative anesthesia, postoperative and obstetric analgesia, and to treat acute radicular pain. Identification of the epidural space is typically carried out using the loss of resistance (LOR) technique, but the usefulness of this technique is limited by false LOR and the inability to reliably detect intravascular or subarachnoid needle placement. In this study, we present a novel epidural needle that allows for the acquisition of optical reflectance spectra from tissue close to the beveled surface. This needle has optical fibers embedded in the cannula that deliver and receive light. With two spectrometers, light received from tissue is resolved across the wavelength range of 500 to 1600 nm. To determine the feasibility of optical tissue differentiation, spectra were acquired from porcine tissues during a *post mortem* laminectomy. The spectra were processed with an algorithm that derives estimates of the hemoglobin and lipid concentrations. The results of this study suggest that the optical epidural needle has the potential to improve the accuracy of epidural space identification.

OCIS codes: (170.3890) Medical optics instrumentation; (170.6510) Spectroscopy, tissue diagnostics; (170.6935) Tissue characterization.

References and links

1. J. M. Neal and J. P. Rathmell, *Complications in Regional Anesthesia & Pain Medicine* (Saunders, 2006).
2. M. K. S. Heran, A. D. Smith, and G. M. Legiehn, "Spinal injection procedures: a review of concepts, controversies, and complications," Radiol. Clin. North Am. **46**(3), 487–514, v–vi (2008).
3. V. L. H. Hoffmann, M. P. Vercauteren, J. P. Vreugde, G. H. Hans, H. C. Coppejans, and H. A. Adriaensen, "Posterior epidural space depth: safety of the loss of resistance and hanging drop techniques," Br. J. Anaesth. **83**(5), 807–809 (1999).
4. T. J. M. Lechner, M. G. F. van Wijk, and A. J. J. Maas, "Clinical results with a new acoustic device to identify the epidural space," Anaesthesia **57**(8), 768–772 (2002).
5. O. Ghelber, R. E. Gebhard, S. Vora, C. A. Hagberg, and P. Szmuk, "Identification of the epidural space using pressure measurement with the compuflo injection pump--a pilot study," Reg. Anesth. Pain Med. **33**(4), 346–352 (2008).
6. H. Kalvoy, O. G. Martinsen, and S. Grimnes, "Determination of tissue type surrounding a needle tip by electrical bioimpedance," in *Proceedings of the 30th Annual International Conference of the IEEE Engineering in Medicine and Biology Society* (IEEE, 2008), pp. 2285–2286.
7. W. W. Roberts, O. E. Fugita, L. R. Kavoussi, D. Stoianovici, and S. B. Solomon, "Measurement of needle-tip bioimpedance to facilitate percutaneous access of the urinary and biliary systems: first assessment of an experimental system," Invest. Radiol. **37**(2), 91–94 (2002).

#144484 - $15.00 USD Received 21 Mar 2011; revised 22 Apr 2011; accepted 1 May 2011; published 6 May 2011

8. A. N. Bashkatov, E. A. Genina, V. I. Kochubey, and V. V. Tuchin, "Optical properties of human skin, subcutaneous and mucous tissues in the wavelength range from 400 to 2000 nm," J. Phys. D Appl. Phys. **38**(15), 2543–2555 (2005).
9. U. Utzinger and R. R. Richards-Kortum, "Fiber optic probes for biomedical optical spectroscopy," J. Biomed. Opt. **8**(1), 121–147 (2003).
10. S. M. Latyev, D. V. Shpakov, V. A. Volchkov, E. A. Puisha, and O. Mollenkhauer, "The possibility of identifying the epidural space in anesthesiological practice by optical methods," J. Opt. Technol. **69**(4), 292–294 (2002).
11. C. K. Ting, M. Y. Tsou, P. T. Chen, K. Y. Chang, M. S. Mandell, K. H. Chan, and Y. Chang, "A new technique to assist epidural needle placement: fiberoptic-guided insertion using two wavelengths," Anesthesiology **112**(5), 1128–1135 (2010).
12. G. Kumar and J. M. Schmitt, "Optimal probe geometry for near-infrared spectroscopy of biological tissue," Appl. Opt. **36**(10), 2286–2293 (1997).
13. W. J. Cui, N. G. Wang, and B. Chance, "Study of photon migration depths with time-resolved spectroscopy," Opt. Lett. **16**(21), 1632–1634 (1991).
14. D. Arifler, C. MacAulay, M. Follen, and R. Richards-Kortum, "Spatially resolved reflectance spectroscopy for diagnosis of cervical precancer: Monte Carlo modeling and comparison to clinical measurements," J. Biomed. Opt. **11**(6), 064027 (2006).
15. G. Zonios, L. T. Perelman, V. M. Backman, R. Manoharan, M. Fitzmaurice, J. Van Dam, and M. S. Feld, "Diffuse reflectance spectroscopy of human adenomatous colon polyps *in vivo*," Appl. Opt. **38**(31), 6628–6637 (1999).
16. R. Nachabé, B. H. W. Hendriks, A. E. Desjardins, M. van der Voort, M. B. van der Mark, and H. J. C. M. Sterenborg, "Estimation of lipid and water concentrations in scattering media with diffuse optical spectroscopy from 900 to 1,600 nm," J. Biomed. Opt. **15**(3), 037015 (2010).
17. T. J. Farrell, M. S. Patterson, and B. Wilson, "A diffusion theory model of spatially resolved, steady-state diffuse reflectance for the noninvasive determination of tissue optical properties *in vivo*," Med. Phys. **19**(4), 879–888 (1992).
18. P. R. Bargo, S. A. Prahl, and S. L. Jacques, "Optical properties effects upon the collection efficiency of optical fibers in different probe configurations," IEEE J. Sel. Top. Quantum Electron. **9**(2), 314–321 (2003).
19. K. A. Schenkman, D. R. Marble, E. O. Feigl, and D. H. Burns, "Near-infrared spectroscopic measurement of myoglobin oxygen saturation in the presence of hemoglobin using partial least-squares analysis," Appl. Spectrosc. **53**(3), 325–331 (1999).
20. R. R. Anderson, W. Farinelli, H. Laubach, D. Manstein, A. N. Yaroslavsky, J. Gubeli 3rd, K. Jordan, G. R. Neil, M. Shinn, W. Chandler, G. P. Williams, S. V. Benson, D. R. Douglas, and H. F. Dylla, "Selective photothermolysis of lipid-rich tissues: a free electron laser study," Lasers Surg. Med. **38**(10), 913–919 (2006).
21. J. M. Conway, K. H. Norris, and C. E. Bodwell, "A new approach for the estimation of body composition: infrared interactance," Am. J. Clin. Nutr. **40**(6), 1123–1130 (1984).
22. L. H. Kou, D. Labrie, and P. Chylek, "Refractive indices of water and ice in the 0.65- to 2.5-μm spectral range," Appl. Opt. **32**(19), 3531–3540 (1993).
23. E. K. Chan, B. Sorg, D. Protsenko, M. O'Neil, M. Motamedi, and A. J. Welch, "Effects of compression on soft tissue optical properties," IEEE J. Sel. Top. Quantum Electron. **2**(4), 943–950 (1996).
24. C. Lubawy and N. Ramanujam, "Endoscopically compatible near-infrared photon migration probe," Opt. Lett. **29**(17), 2022–2024 (2004).
25. M. A. Reina, C. D. Franco, A. López, J. A. Dé Andrés, and A. van Zundert, "Clinical implications of epidural fat in the spinal canal. A scanning electron microscopic study," Acta Anaesthesiol. Belg. **60**(1), 7–17 (2009).
26. W. F. Cheong, S. A. Prahl, and A. J. Welch, "A review of the optical properties of biological tissues," IEEE J. Quantum Electron. **26**(12), 2166–2185 (1990).
27. W. G. Zijlstra, A. Buursma, and A. Zwart, "Molar absorptivities of human hemoglobin in the visible spectral range," J. Appl. Physiol. **54**(5), 1287–1291 (1983).
28. W. Verkruysse, G. W. Lucassen, J. F. de Boer, D. J. Smithies, J. S. Nelson, and M. J. C. van Gemert, "Modelling light distributions of homogeneous versus discrete absorbers in light irradiated turbid media," Phys. Med. Biol. **42**(1), 51–65 (1997).
29. D. J. Marcinek, C. E. Amara, K. Matz, K. E. Conley, and K. A. Schenkman, "Wavelength shift analysis: a simple method to determine the contribution of hemoglobin and myoglobin to *in vivo* optical spectra," Appl. Spectrosc. **61**(6), 665–669 (2007).
30. R. Nachabé, B. H. Hendriks, M. van der Voort, A. E. Desjardins, and H. J. C. M. Sterenborg, "Estimation of biological chromophores using diffuse optical spectroscopy: benefit of extending the UV-VIS wavelength range to include 1000 to 1600 nm," Biomed. Opt. Express **1**(5), 1432–1442 (2010).
31. N. V. Iftimia, B. E. Bouma, M. B. Pitman, B. Goldberg, J. Bressner, and G. J. Tearney, "A portable, low coherence interferometry based instrument for fine needle aspiration biopsy guidance," Rev. Sci. Instrum. **76**(6), 064301 (2005).
32. J. G. Wu, M. Conry, C. H. Gu, F. Wang, Z. Yaqoob, and C. H. Yang, "Paired-angle-rotation scanning optical coherence tomography forward-imaging probe," Opt. Lett. **31**(9), 1265–1267 (2006).
33. D. T. Raphael, C. H. Yang, N. Tresser, J. G. Wu, Y. P. Zhang, and L. Rever, "Images of spinal nerves and adjacent structures with optical coherence tomography: preliminary animal studies," J. Pain **8**(10), 767–773 (2007).

#144484 - $15.00 USD Received 21 Mar 2011; revised 22 Apr 2011; accepted 1 May 2011; published 6 May 2011

1. Introduction

Accurate navigation of the needle tip is critical for safe and effective use of regional anesthesia. The most common technique for identifying the epidural space is the loss of resistance (LOR) technique, which relies on the operator to detect an abrupt change in resistance to injection as an advancing needle passes through the ligamentum flavum and into the epidural space. However, changes in resistance to injection can occur if the needle strays from midline before it reaches the ligamentum flavum and the epidural space, and a lack of firm resistance to injection occurs in some patients even when the needle tip is seated in ligament. Both of these problems hinder accurate identification of the epidural space using the LOR technique. An additional limitation of the LOR technique is that it cannot accurately identify when the needle passes into a vascular structure such as an epidural vein. While fluoroscopic guidance has been described as a means to improve the accuracy of epidural needle placement, the use of fluoroscopy with radiographic contrast is not suitable in many settings [1,2]. Localization of the epidural space remains challenging in large part due to uncertainties about the type of tissue that lies just ahead of the needle tip.

Many methods for sensing tissue properties at the needle tip have been proposed to improve the accuracy of epidural space identification. Certain methods have exploited the negative pressure within the epidural space, including the “hanging drop” method. This method has been shown to be associated with an increased risk of inadvertent dural puncture relative to the LOR technique [3] and is not widely used. An alternate method involves quantifying the pressure at the needle tip and providing auditory and visual displays of the pressure waveforms as a means to detect the passage of the needle tip through the ligamentum flavum [4]. While promising, this method still relies on the presence of a dense ligamentum flavum and thus may not be sufficient for preventing complications such as dural puncture that result from advancement of the needle too far within the epidural space. Yet another method involves a computerized injection pump that controls the rate of saline infusion and monitors pressures at the injection site; the epidural space is identified by a sustained pressure decrease [5]. However, the expected pressure in the epidural space is often not well established, particularly in patients who have undergone back surgery and those who are morbidly obese. Recently there has been interest in utilizing bioimpedance, a measure of the opposition to alternating current, to discriminate between tissues at the needle tip. In preliminary studies, it was shown that several types of tissue could be discriminated, including muscle and fat [6]. It has been suggested that the epidural space could be located with this method, but this method has yet to undergo testing [7].

Spectrophotometric measurements using visible and near-infrared light can readily differentiate tissues based on differences in optical absorption, and as such, they could allow for differentiating tissues in the vicinity of the epidural space. In particular, diffuse reflectance spectroscopy (DRS) can identify differences in the volume fractions of chromophores such as hemoglobin, water, and lipid, which are known to vary between tissue types [8]. A variety of different needle-sized DRS probes have been developed for tissue differentiation [9]. Latyev et al. described in general terms the potential for inclusion of optical lightguides in epidural needles and for optical identification of the epidural space; however, they did not present optical measurements from tissues [10]. Recently, optical identification of the epidural space with a porcine model was demonstrated [11]. A custom stylet with integrated optical fibers, positioned in a Tuohy needle, was used to deliver and receive light; the epidural space was differentiated from the ligamentum flavum based on the ratio of reflectivities at 650 nm and at 532 nm. Whilst this ratio has the advantage of simplicity, it remains to be determined how optical signals acquired from the stylet correspond to the physiological parameters of tissue. Additionally, with the two chosen wavelengths, it is likely that little optical contrast was generated from lipids, which are present in high concentrations in the epidural space.

In this study, we present an epidural needle with optical fibers embedded in the cannula and an optical console comprising two spectrometers that resolved light across both visible and near-infrared wavelength ranges. Spectra were acquired from tissue adjacent to the

#144484 - $15.00 USD Received 21 Mar 2011; revised 22 Apr 2011; accepted 1 May 2011; published 6 May 2011

beveled surface, and processed with a custom algorithm that derived volume fractions of prominent chromophores.

2. Materials and methods

2.1. Optical epidural needle

The epidural needle was derived from the geometry of an 18-gauge commercial Quincke needle (Becton, Dickinson and Company, Franklin Lakes, NJ, USA). The beveled surface of the needle cannula (NC) was angled at 20 degrees with respect to the needle axis (Fig. 1). Three optical fibers were embedded in the cannula with epoxy and polished so that their distal ends were flush with the beveled surface. One fiber was located near the distal end of the beveled surface and delivered light to tissue. Two other optical fibers in close proximity to each other (central axis separation: 0.37 mm) were located at the proximal end of the beveled surface and received light scattered within tissue. The central axes of the distal and proximal optical fibers were separated from each other by 2.4 mm. Fiber separations of 2-5 mm have been shown to be optimal for measuring chromophore volume fractions in the presence of a variable scattering background [12]. The low-hydroxyl, silica-silica optical fibers (Ocean Optics, Denudin, Florida, USA) were 220 microns in diameter after the buffer was stripped at the distal end, with 200 micron cores and a numerical aperture of 0.22. With each fiber polished to match the steep angle of the beveled surface, light initially underwent total-internal reflection at the fiber/tissue interface and subsequently reflected from the metallic surface that surrounded the fiber before exiting this interface and entering the tissue.

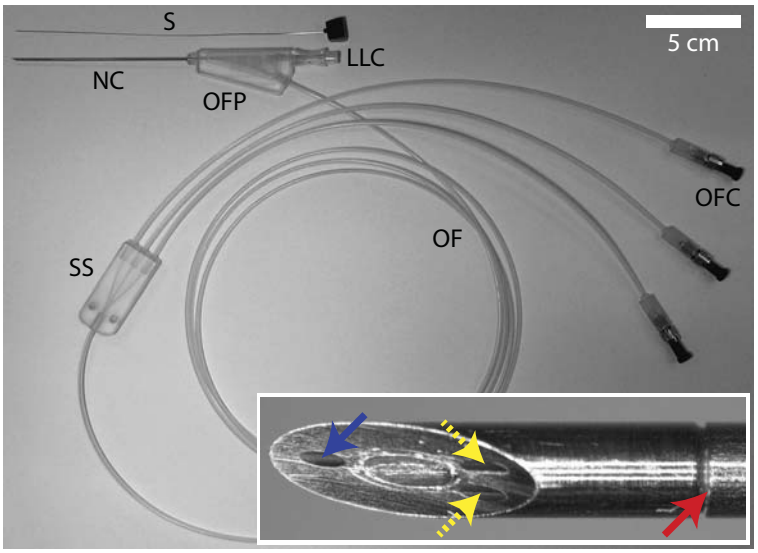

Fig. 1. Spinal needle with integrated optical fibers and stylet (S). Proximal to the needle cannula (NC), optical fibers exit via a port (OFP) beneath the female Luer Lock connector (LLC). A sheath splitter (SS) separates the sheath connected to the proximal end into three individual sheaths; the optical fibers (OF) contained individually within the latter sheaths ultimately terminate at connectors (OFC). A close-up, en face view of the beveled surface (figure insert) shows the distal ends of the optical fibers that deliver light to tissue (blue solid arrow) and receive light from tissue (yellow dashed arrows), and the junction between the tip and the proximal part of the cannula (red solid arrow).

The proximal part of the NC, connected to the tip with epoxy, consisted of two concentric tubes that enclosed the optical fibers. The outer and inner diameters of the NC were 1.3 mm and 0.4 mm, respectively. As such, the outer diameter was consistent with that of a typical 18-gauge needle. The stylet—the removable insert within the cannula—was constructed from a solid rod with its tip polished at an angle of 20 degrees to match the angle of the beveled

#144484 - $15.00 USD Received 21 Mar 2011; revised 22 Apr 2011; accepted 1 May 2011; published 6 May 2011

surface of the NC. All metal components comprised by the needle tip and cannula were constructed from stainless steel.

At the proximal end of the needle, a standard plastic female Luer Lock connector allowed for connections with syringes. A corresponding connector was fitted onto the stylet. The optical fibers exited the NC at a plastic port. Outside the needle, the three optical fibers were protected with a flexible, plastic protective sheath until their termination at SMA connectors.

2.2. Console

The epidural needle was optically connected to a custom console that delivered and received light. A tungsten-halogen source with an integrated shutter (Ocean Optics, HL-2000-HP) in the console was coupled to the delivery fiber. Light was received from the epidural needle by the console via the two collection optical fibers. In the console, each collection fiber was directed to a different spectrometer; both spectrometers comprised the same type of compact spectrograph (Shamrock 163, Andor Technology, Belfast, United Kingdom). Spectrometer 1 resolved light in the 500 to 1000 nm range, with detection provided by a silicon array (DU420A-BR-DD, Andor Technology, Belfast, United Kingdom). Spectrometer 2 resolved light in the 900 to 1600 range, with detection provided by an InGaAs sensor array (DU492A-1.7, Andor Technology, Belfast, United Kingdom). Both sensors were cooled to −50 degrees Celsius during operation to minimize dark currents. With both spectrometers, the spectral resolution was approximately 7 nm.

Spectra from both spectrometers were acquired simultaneously using a custom program written in Labview (National Instruments Corporation, Austin, Texas, USA). Spectral processing was performed offline, with custom software written in Matlab (The Mathworks, Natick, Massachusetts, USA). The pre-processing steps consisted of: 1) wavelength calibration; 2) background subtraction; 3) intensity calibration; 4) spectral filtering. Background subtraction was performed with a spectrum acquired with the light source shuttered. A calibrated reflectance standard (WS-1-SL, Labsphere, North Sutton, New Hampshire, USA) was used for intensity calibration: prior to insertion of the needle within tissue, the needle tip was positioned 1.57 mm above the reflectance standard with the needle facet parallel to the surface of the standard. Intensity calibration consisted of division with respect to the background-subtracted spectrum acquired from the reflectance standard.

Light that was delivered to the tissue scattered before reaching the collection fiber. The average maximum distance from the beveled surface reached by photons that entered the collection fiber depended on the optical properties of the tissue such as the scattering and absorption coefficients and the anisotropy parameter [13], all of which are wavelength-dependent. While detailed simulations of light paths encountered for different tissues are beyond the scope of this study, it can be estimated from the results of Arifler et al. [14] that for the case where the needle is in contact with epithelial and stromal tissue, the “look-ahead” distance of the needle was approximately 1.2 mm for 500 nm incident light.

2.3. Laminectomy

Optical measurements with the needle were acquired from the spinal region of a Swedish Landrace swine (42 kg; female). The tissue was obtained after the swine had been sacrificed following experiments that were part of a different study. The laminectomy commenced immediately post-mortem, centered in the lower lumbar region (L1-L2). As different tissue layers were exposed during the course of the laminectomy, spectra were acquired with the beveled surface in contact with tissue (Fig. 2). For each type of tissue, 10 spectra were acquired. During acquisition of spectra, the needle was held manually; efforts were made not to compress tissue and to maintain the needle in fixed positions. In the case where spectra were obtained from the spinal cord surface, the beveled surface was positioned so that it was not in direct contact with the arterial plexus.

#144484 - $15.00 USD Received 21 Mar 2011; revised 22 Apr 2011; accepted 1 May 2011; published 6 May 2011

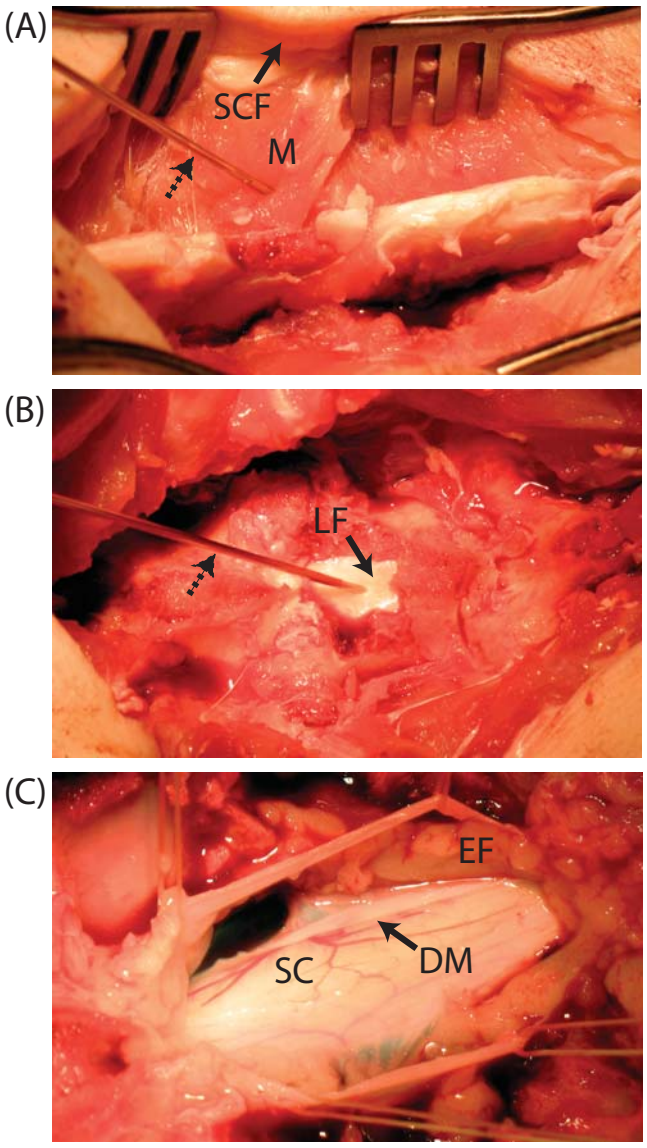

Fig. 2. Laminectomy performed at the L1-L2 level of a swine, in which optical spectra were acquired with the needle/optical probe. After retracting subcutaneous fat (SCF) and muscle (M) layers (A), the smooth white surface of the ligamentum flavum (LF) was exposed (B). With the ligamentum flavum retracted (C), epidural fat (EF) with a yellow appearance was visible above the dura mater (DM). Beneath the dura mater, the surface of the spinal cord (SC) and the associated vascular plexus was visible. The needle is identified in (A) and (B) with dashed arrows.

2.4. Spectral Processing Algorithm

Obtaining quantitative estimates of chromophore volume fractions from diffuse reflectance spectra is a well-studied inverse problem in the field of biomedical optics. The spectral processing algorithm utilized a computational model of light propagation for this purpose. The model accepted chromophore volume fractions and light scattering parameters as input and generated a spectrum as output. Estimates were revised iteratively to minimize the difference between the spectrum generated by the model and that acquired from tissue. This solution was first developed to analyze spectra acquired from colon polyps [15] and was recently modified

#144484 - $15.00 USD Received 21 Mar 2011; revised 22 Apr 2011; accepted 1 May 2011; published 6 May 2011

to include absorption by lipids in a study by Nachabé et al. [16], which included validation with tissue phantoms. The light propagation model consisted of an analytic diffusion model with a single source, which expressed the intensity of light received from tissue as a function of two wavelength-dependent optical properties: the absorption and reduced scattering coefficients [17]. It was assumed that the tissue regions from which the spectra derived were optically homogeneous. In this study, the absorption coefficient was modeled as a linear sum of the absorption coefficients of the dominant chromophores; the reduced scattering coefficient was modeled as a power law [18]. The light propagation model was applied separately to the spectra obtained from the two spectrometers. For spectra in the range of 500 to 1000 nm obtained from spectrometer 1, the dominant chromophores were assumed to be oxy- and deoxy-hemoglobin. For spectra in the range of 900 to 1600 nm obtained from spectrometer 2, the dominant chromophores were assumed to be water and lipid. With the aforementioned iteration method, two parameters were estimated: the blood fraction and the lipid fraction. The former parameter is defined as the estimated total hemoglobin volume fraction, expressed as a percentage of the concentration of hemoglobin in normal human blood (150 g/liter, the average hemoglobin concentration in whole blood). The latter parameter is defined as the estimated concentration of lipid normalized by the sum of the estimated concentrations of lipid and water.

3. Results

Spectra acquired from tissues exposed during the laminectomy are displayed as the intensity of light received from tissue as a function of the wavelength (Fig. 3). They exhibited several prominent absorption peaks, which manifested as lower signal intensities within specific wavelength ranges. In all spectra, absorption peaks were observed for wavelengths in the range of 500 to 600 nm, which was consistent with the presence of hemoglobin [19]. In the case of spectra acquired from subcutaneous fat and skeletal muscle, a single minimum in intensity at 557 nm was observed within this range; for spectra acquired from other tissues, two minima were observed near 542 nm and 576 nm. These minima were consistent with the presence of deoxygenated and oxygenated forms, respectively; a small absorption peak centered at 757 nm is also associated with the presence of the deoxygenated form of hemoglobin.

Absorption peaks at 1210 nm were present in all spectra except for those acquired from skeletal muscle. These absorption peaks are consistent with the presence of lipids [20]. A smaller absorption peak at 930 nm, consistent with the presence of lipid [21], was visible in spectra that exhibited prominent absorption peaks at 1210 nm. The lipid absorption peaks were particularly prominent in spectra acquired from subcutaneous and epidural fat; they were visually absent in those acquired from skeletal muscle. The prominent and broad absorption peak centered at 1455 nm and the less prominent ones at 976 and 1197 nm were consistent with the presence of water [22].

Blood and lipid fractions derived with the spectral processing algorithm were found to have both differences and similarities across tissue types (Fig. 4). Similar blood fractions were obtained from epidural fat and skeletal muscle; they were approximately two-fold higher than those obtained from the intervening tissue, the ligamentum flavum. The mean blood fraction obtained from epidural fat was 1.2-fold higher than that obtained from the dura mater and 1.9-fold higher than that obtained from the spinal cord. The lipid fraction obtained from epidural fat was 25-fold higher than that obtained from skeletal muscle, and 1.2-fold higher than that obtained from the surface of the ligamentum flavum. The mean lipid fraction obtained from epidural fat was more than two-fold greater than those obtained from the dura mater and from the spinal cord. Intensity variations in spectra, which are displayed as standard deviations relative to the mean in Fig. 4, were greatest overall in spectra acquired from subcutaneous fat and from the spinal cord surface. Intensity variations can arise from differences in pressure that are applied by the needle [23].

#144484 - $15.00 USD Received 21 Mar 2011; revised 22 Apr 2011; accepted 1 May 2011; published 6 May 2011

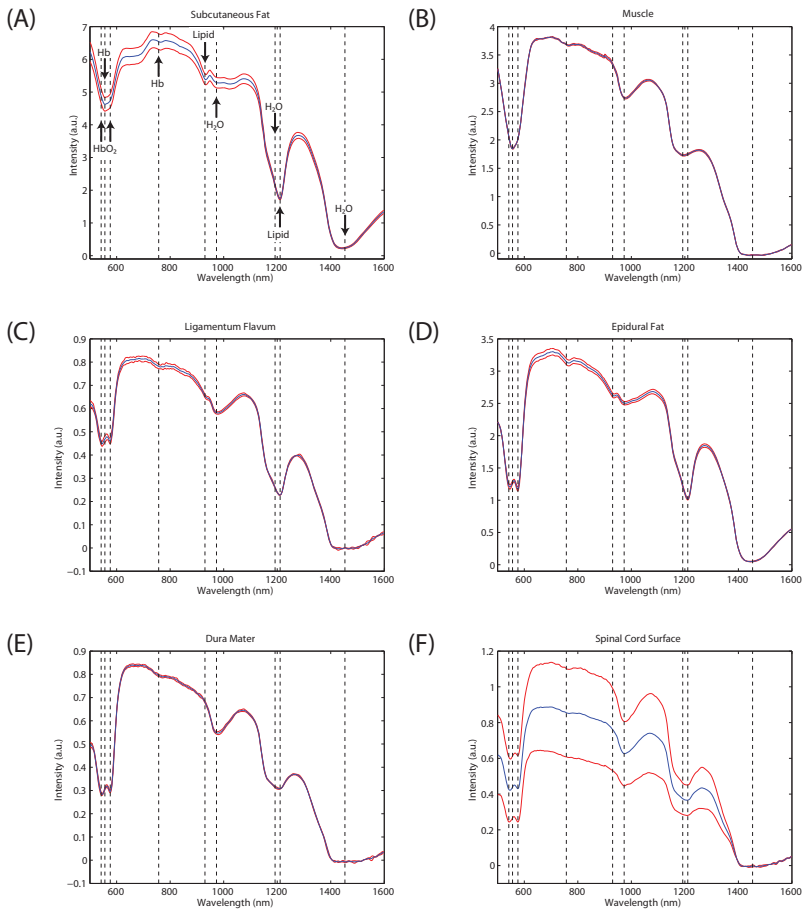

Fig. 3. Spectra acquired from tissues exposed during the laminectomy: (A) subcutaneous fat; (B) muscle; (C) ligamentum flavum; (D) epidural fat; (E) dura mater; (F) spinal cord surface. From each location, 10 spectra were acquired; they are displayed as mean (blue) ± SD (red). Specific wavelengths corresponding to selected absorption peaks are indicated with dashed lines. Oxy-hemoglobin: 542 and 576 nm; deoxy-hemoglobin: 557 and 757 nm; lipids: 930 and 1210 nm; water: 976, 1197, and 1455 nm.

4. Discussion

Our preliminary experience suggested that the optical fiber connection to the console did not significantly restrict manipulation of the needle, as it was light and flexible. Future needle designs could incorporate larger inner cannula diameters if smaller optical fibers are used. Future optical epidural needles could also incorporate different geometries to derive spectra from tissue regions at different distances from the needle tip. All other factors being equal, needles with larger inter-fiber distances have correspondingly larger look-ahead distances. While that may be desirable for early identification of tissues ahead of the needle tip, problems with interpreting spectra may arise if the inter-fiber distance is too large so that multiple tissue layers are sampled. If the inter-fiber distance is too small, the depth of the absorption peaks may be too small to provide robust detection of certain chromophores that exhibit relatively low absorption.

The optical epidural needle in this study was designed to derive spectroscopic contrast from tissues at the point of injection. The needle design could be modified to derive spectra from tissues surrounding the sharp tip, which could be valuable for determining whether the needle is close to puncturing a blood vessel. Such models could extend the paradigm of

#144484 - $15.00 USD Received 21 Mar 2011; revised 22 Apr 2011; accepted 1 May 2011; published 6 May 2011

sensing at the beveled tip to include side-facing optical fibers that detect light incident on the NC [24].

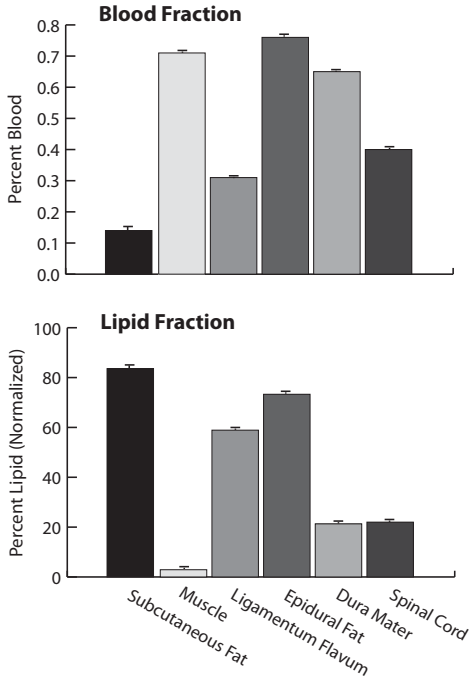

Fig. 4. Blood and lipid fractions obtained with the spectral processing algorithm from tissues exposed during the laminectomy. From each tissue, 10 spectra were acquired; the corresponding blood and lipid fractions are displayed as mean ± SD.

Given that the data were acquired from only a few locations in a single cadaveric specimen, the observed differences in the blood and lipid fractions provide only an initial indication of the variability of these parameters that could be encountered in different clinical contexts. We anticipate that measurements acquired *in vivo* will reveal considerable intra-tissue variability. Tissue heterogeneity can be expected to contribute to this variability, as can the occasional presence of additional tissues within the look-ahead distance of the needle. Additionally, minor bleeding events could result in the presence of small volumes of blood that remain close to the bevel surface and alter the spectroscopic signals and blood fractions. The extent to which this would occur during *in vivo* insertions is unknown. In this study, variations in the pressure imparted by the needle on tissues likely resulted in corresponding variations in the shapes and intensities of the spectra, but it is unclear whether this effect can completely account for the large variations in the spectra acquired from subcutaneous fat and from the surface of the spinal cord.

The spectral processing algorithm that was used in this study has several limitations. First, it implicitly involves the assumption that the region of tissue from which a spectrum derives is homogeneous. This assumption is likely to be violated in several cases, including situations where spectra are acquired from thin tissue layers such as the dura mater. Second, it accounts for only four chromophores that are known to give rise to prominent absorption peaks. Follow-up studies are required to determine how accurately the volume fractions of additional chromophores such as carotenes, which are known to be present in epidural fat [25], can be estimated. The spectral processing algorithm was designed to account for differences in the magnitude and wavelength-dependence of the reduced scattering coefficient, under the assumption that the reduced scattering coefficient is much greater than the absorption coefficient [16]. This assumption is valid for most biological tissues in the visible and near-

#144484 - $15.00 USD Received 21 Mar 2011; revised 22 Apr 2011; accepted 1 May 2011; published 6 May 2011

infrared regions of the spectrum [26]; in cases when it is not valid, the derived blood and lipid parameters may be inaccurate.

Accurately measuring the blood fraction involves several challenges. In the spectral processing algorithm, small differences in the optical absorption of hemoglobin relative to human forms [27] were discounted. As hemoglobin is located in erythrocytes, its distribution in tissues is inhomogeneous at the cellular and vascular level. These inhomogeneities likely had small but measurable effects on the spectra [28] that are not accounted for in the spectral processing algorithm. With optical reflectance spectra obtained from skeletal muscle, absorption from myoglobin may be prominent; as such, it could confound estimation of the blood fraction [29]. Future spectral processing algorithms that account for the aforementioned challenges, including ones that incorporate hemoglobin packaging parameters [30], could potentially provide accurate estimates of hemoglobin oxygen saturation and could therefore distinguish between arterial and venous blood. Another challenge encountered in the context of this *ex vivo* study was the potential contamination of tissues with blood released during the course of the laminectomy; the presence of this additional blood may have elevated the measured blood fractions.

Currently, there are several methods for optically imaging within the epidural space to acquire information that is not available from the LOR technique or from fluoroscopy. With epiduroscopy, tissue ahead of the needle is visualized directly, typically by means of a flexible fiber bundle and fiber-optic illumination. This method is time-consuming and cumbersome, requiring placement of a large introducer cannula and continuous infusion of saline to distend the epidural space and create a clear path for visualization through the epiduroscope. Epiduroscopy images can be difficult to interpret, and the method is completely impractical for routine purposes like providing epidural anesthesia. Optical coherence tomography (OCT), an optical analog of ultrasound, provides micron-level spatial resolution and does not require a saline bolus for imaging within the epidural space; images can be generated with probes in direct contact with tissue [31,32]. In a preliminary study, Raphael et al. demonstrated that a forward-looking OCT probe could resolve structures such as arteries and nerves in a porcine model and a dural puncture in a rabbit [33]. At present, the histological correlates of OCT images acquired from the spinal region are not well understood, and more studies are required to determine whether OCT can provide sufficient image contrast for structures relevant to decreasing complications resulting from epidural injection.

5. Conclusion

This study demonstrated the feasibility of obtaining optical reflectance spectra from tissues encountered during epidural injections, with optical fibers integrated into the cannula of an epidural needle of a size and configuration that would allow its practical use during regional anesthesia. Based on this work, future *in vivo* studies could determine what absolute or relative changes in blood and lipid fractions are optimal for identifying the epidural space. We conclude that this optical epidural needle has the potential to improve the accuracy of needle placement during epidural injections by providing information about the location of the needle tip that is complementary to that obtained from the LOR technique and from fluoroscopic images.

Acknowledgments

The authors gratefully acknowledge assistance with animal experiments by Pellina Janson at Karolinska University Hospital, and assistance with needle and console design by colleagues at Philips Research and VDL: Frans van Gaal, Ben Wassink, Henk Compen, Cor van der Vleuten, Jean Schleipen, and Martin Vernhout.

#144484 - $15.00 USD Received 21 Mar 2011; revised 22 Apr 2011; accepted 1 May 2011; published 6 May 2011